Research Paper

Fetal–maternal interface impedance parallels local NADPH oxidase related superoxide production

L. Guedes-Martins [a,b,c,d,*], E. Silva [a,b,c], A.R. Gaio [e,f], J. Saraiva [a,b,c,d], A.I. Soares [a,b,c], J. Afonso [g], F. Macedo [h], H. Almeida [a,b,c,i]

[a] Department of Experimental Biology, Faculty of Medicine, University of Porto, 4200-319 Porto, Portugal
[b] IBMC-Instituto de Biologia Molecular e Celular, 4150-180 Porto, Portugal
[c] Instituto de Investigação e Inovação em Saúde, Universidade do Porto, 4200-319 Porto, Portugal
[d] Centro Hospitalar do Porto EPE, Departamento da Mulher e da Medicina Reprodutiva, Centro Hospitalar do Porto EPE, Largo Prof. Abel Salazar, 4099-001 Porto, Portugal
[e] Department of Mathematics, Faculty of Sciences, University of Porto, Rua do Campo Alegre, 4169-007 Porto, Portugal
[f] CMUP-Centre of Mathematics of the University of Porto, Rua do Campo Alegre, 4169-007 Porto, Portugal
[g] Department of Pharmacology, Faculty of Medicine, University of Porto, 4200-319 Porto, Portugal
[h] Department of Cardiology, Faculty of Medicine, University of Porto, 4200-319 Porto, Portugal
[i] Obstetrics-Gynecology, Hospital-CUF Porto, 4100 180 Porto, Portugal

ARTICLE INFO

ABSTRACT

Blood flow assessment employing Doppler techniques is a useful procedure in pregnancy evaluation, as it may predict pregnancy disorders coursing with increased uterine vascular impedance, as pre-eclampsia. While the local causes are unknown, emphasis has been put on reactive oxygen species (ROS) excessive production. As NADPH oxidase (NOX) is a ROS generator, it is hypothesized that combining Doppler assessment with NOX activity might provide useful knowledge on placental bed disorders underlying mechanisms.

A prospective longitudinal study was performed in 19 normal course, singleton pregnancies. Fetal aortic isthmus (AoI) and maternal uterine arteries (UtA) pulsatility index (PI) were recorded at two time points: 20–22 and 40–41 weeks, just before elective Cesarean section. In addition, placenta and placental bed biopsies were performed immediately after fetal extraction.

NOX activity was evaluated using a dihydroethidium-based fluorescence method and associations to PI values were studied with Spearman correlations. A clustering of pregnancies coursing with higher and lower PI values was shown, which correlated strongly with placental bed NOX activity, but less consistently with placental tissue.

The study provides evidence favoring that placental bed NOX activity parallels UtA PI enhancement and suggests that an excess in oxidation underlies the development of pregnancy disorders coursing with enhanced UtA impedance.

© 2015 The Authors. Published by Elsevier B.V. This is an open access article under the CC BY-NC-ND license (http://creativecommons.org/licenses/by-nc-nd/4.0/).

Introduction

In recent years, the range of ultrasound applications for the study of blood flow has increased remarkably due to device improvements, extensive and reliable data collection, and the non-invasive nature of the procedure. In particular, Doppler effect assessment of the impedance of fetal and placental circulation has become a routine operation during pregnancy evaluation and a necessary tool in screening for impaired utero-placental circulation [1,2].

Over the course of a pregnancy, remarkable circulatory changes occur in the pelvis: on the one side is a developing foetus with

enhanced nutritional demands, whereas on the other side, uterine circulation has to adapt continuously to cope with such demands. These distinct features make the uteroplacental interface a crucial site of circulation whose impedance can be assessed by approaching the aortic isthmus (AoI) on the fetal side and the uterine arteries (UtA) on the maternal side. In this respect, although different impedance parameters may be employed, emphasis has been placed on the pulsatility index (PI) because of its ability to better describe the velocity waveform [3,4].

During prenatal life, the parallel position of both cardiac ventricles assigns a special position to the AoI, as it reflects the balance of the functional accomplishments and the individual territorial impedances of the two ventricles [4,5]. Thus, the direction of blood flow in the aortic isthmus will depend on the relative difference between the upper body and the subdiaphragmatic circulation supplying the lower body and placenta [6]. Abnormal flow patterns in the AoI, identified by high impedance values, have been shown to be associated with fetal circulatory redistribution [6–10]; in addition, routine AoI Doppler assessment has been shown to predict perinatal and long-term neurodevelopmental outcomes in placental insufficiency [6,11,12]. Indeed, the value of AoI blood flow assessment has been emphasized as changes in AoI antedate umbilical artery findings [7].

On the mother's side, a normal uterine artery waveform reflects successful vascular remodelling at the uterine placental bed that includes the decidua and part of the myometrium [13,14]. In early pregnancy, the UtA Doppler waveform exhibits a rapid increase and decrease in systolic flow velocity that is followed by a notch in the early diastole [15,16]. This feature, which usually recedes as the pregnancy progresses [3,16] contributes to a mean diastolic velocity rise and a UtA-PI value reduction [3,17]. Interestingly, in a group of unselected pregnant women at 22–24 weeks, enhanced uterine artery PI was reported to have a 69% sensitivity for pre-eclampsia (PE) and the appearance of intra-uterine growth restriction (IUGR) in the following weeks, a value that rose to 83% in cases of protodiastolic notch persistence [18]. Although the detection rate of PE as a result of enhanced UtA-PI was found to be superior to the use of a patient's epidemiological data [19], additional conditions must be met. Other reports have indicated that abnormal UtA impedance at 22 weeks and PE establishment were significantly correlated only in the case of poor fetal outcome, including IUGR and preterm birth [20,21]. More recently, top decile PI values and bilateral notching were considered to have good predictive value for enhanced risk of stillbirth resulting from placental factors [22]. As a corollary favouring the relevance of UtA Doppler impedance, an extensive meta-analysis [23] concluded that an enhanced second trimester PI combined with a notch was a good predictor of PE in low- and high-risk patients and of severe IUGR in low-risk patients. Moreover, the findings supported the recommendation to employ PI and notching uterine artery assessment in daily clinical practice [23]. Most of the referred obstetrical adverse conditions were recognized to result from abnormal placental bed remodelling [14], but despite a wealth of structural information, there is still insufficient knowledge regarding local regulation during placentation.

The involvement of the process of biological oxidation was proposed. The local, continued production of reactive oxygen species (ROS) is a cellular requirement that, in small and balanced amounts, appears to exert a beneficial role on normal pregnancies. This context is relevant to the effect of ROS generated by NADPH oxidase (NOX) activity in the uterus and placenta where, through the activation of NF-κB, they regulate local angiogenesis [24,25] and play a relevant role in normal placental bed establishment.

By contrast, excessive ROS production results in oxidatively stressful conditions, inflammation, circulatory derangement, and placental bed cell apoptosis or necrosis. These events may occur transiently during labour in a fashion consistent with ischaemia-reperfusion injury [26]; when lasting longer, or throughout the pregnancy, they may result in placental function impairment [27,28] and serious pregnancy complications [24,28].

Despite the likelihood of the process of ROS production, the identity and contribution of the redox players involved have remained unknown. To gain a better understanding, it is reasonable to address putative contributors as part of a wider approach. Therefore, we hypothesize that redox status, measured as the NOX activity at the placental bed and in the placenta, relates to blood flow impedance measured at the fetal aortic isthmus and at the maternal uterine arteries.

Materials and methods

Subjects

This study was approved by the local ethics committee of Centro Hospitalar do Porto–Unidade Maternidade Júlio Dinis and all subjects provided written informed consent [IRB protocol number: 133/10 (086-DEFI/126-CES)]. The methods were performed in accordance with the approved guidelines.

The study was performed from January 2010 to December 2013. Inclusion criteria were: healthy normotensive parturient with singleton term pregnancies and gestational age ≥ 40 weeks, scheduled for elective cesarean section under spinal anesthesia due to fetal breech presentation, suspected cephalopelvic disproportion, or previous caesarean. Acceptable medications were folic acid, vitamins, and iron supplements.

Exclusion criteria were: patients in labour or with ruptured membranes; those with multiple gestations, coagulopathy, diabetes, or any pregnancy-induced hypertension including pre-eclampsia; and those receiving β-tocolytic drugs.

Gestational age was calculated by the crown-rump length between 11 and 14 weeks [29] by several experienced sonographers from the Prenatal Diagnosis Department of our institution.

On the day of caesarean section, biometrical data were collected and the patients were observed by a senior specialist who also reviewed their medical records.

The subarachnoid block was performed in the surgical suite using a combined needle-through-needle spinal-epidural technique (typical for caesarean section at our institution) with an epidural 18-G Tuohy needle and 27-G subarachnoid pencil point needle. Spinal anesthesia comprised 8–9 mg of hyperbaric bupivacaine (5 mg/ml) and 2–2.5 μg sufentanil (5 μg/ml) administered intrathecally, targeting the T4-S4 dermatomes.

The healthy condition of the infant was determined through examination by a neonatologist at birth and 1 month after birth.

Doppler flow assessment

Ultrasound examinations were performed using Voluson 730 Pro (GE Healthcare Technologies, Milwaukee, WI, USA) ultrasound equipment containing multifrequency transabdominal transducers (GE Healthcare Probe Type RAB4-8L) at any time of the day, during the second trimester routine scan (first time point), and immediately before the intrathecal blockade (second time point) for caesarean section.

All measurements were performed by a single experienced investigator (L.G-M; 6 years of experience in obstetric and gynaecologic ultrasound) to minimize inter-observer variability. Intra-observer reliability was estimated from two consecutive readings of the pulsatility indexes in the UtA and AoI. Smokers

were required to abstain from smoking for at least 2 h prior to examination.

For uterine artery evaluation, the probe was placed on the lower abdominal quadrants and angled medially, and color Doppler imaging was used to localize the uterine artery as it crossed over the external iliac artery. In all cases, an angle less than 30° was assured before the pulsed Doppler probe was placed over the entire vessel width. Angle correction was then applied, and the signal was updated until three similar consecutive waveforms were found to calculate the left and right uterine artery pulsatility indexes using the device software. The mean UtA-PIs in the left and right arteries were then determined.

For AoI evaluation, all recordings used for measurements were sampled from the longitudinal aortic arch and performed in the absence of fetal movements. The scanning plane was adjusted to obtain an insonation angle $< 30°$. The filter was set at 50 Hz and the energy output levels used were lower than 50 mW/cm^2.

Placenta and placental bed biopsies

Biopsies of the placenta and placental bed were performed by open biopsy during caesarean section immediately after fetal extraction and prior to oxytocin administration. Using tissue scissors, two fragments approximately 10×5 mm^2 (width $\times$ depth) were obtained. The first fragment was collected from the placental bed and the second was obtained from the central area of the placental maternal surface. In individual cases, because of a small uterine bleeding site, we proceeded to haemostasis control using an isolated absorbable synthetic suture (Polyglactin 910, 2/0). After collection under aseptic conditions, the samples were briefly washed in saline solution and immediately frozen in liquid nitrogen before being stored at -80 °C.

Dihydroethidium conversion

$O_2^{\bullet-}$ production from NADPH oxidase was evaluated using a dihydroethidium (DHE)-based fluorescence method [30,31]. DHE is used in fluorimetric detection assays because upon reaction with superoxide anions, it is converted to 2-hydroxyethidium, following DNA intercalation, emits red fluorescence.

Placenta and placental bed samples were homogenized in a glass-to-glass homogenizer in cold HEPES buffer (25 mM) containing EDTA (1 mM) and phenylmethyl-sulfonyl fluoride (PMSF) (0.1 mM). Protein content was assayed by the Bradford method [32] and 12.5 μg of homogenate were used for the assay. Tissue homogenates were incubated in HEPES/EDTA buffer with DHE (20 μM), salmon testes DNA (0.5 mg/ml), and NADPH (1 mM). Superoxide dismutase (200 U/ml) was used to confirm the specificity of the method. To determine whether NADPH oxidase was the source of $O_2^{\bullet-}$ an inhibitor of NOX (diphenylene iodonium, DPI, 500 μM) was used. The effects of a xanthine oxidase inhibitor (oxipurinol, 500 μM) and a nitric oxide synthase inhibitor (nitro-L-arginine methylester, L-NAME, 500 μM) were also evaluated to exclude other possible contributors for the $O_2^{\bullet-}$ 2-hydroxyethidium mediated fluorescence [Supplementary Fig. S1]. It was thus demonstrated that, under the experimental conditions used, the observed increase in fluorescence is mainly due to NOX activity; as such, DHE conversion will be considered an indicator of NOX activity. The reaction was followed for 15 min at 37 °C. Fluorescence was measured in a final volume reaction of 200 μl at 480 nm-excitation and 580 nm-emission using a fluorescence microplate reader (Spectramax Gemini, Molecular Devices, Sunnyvale, CA, USA). The results were expressed as fluorescence arbitrary units per 15 min per 12.5 μg of protein.

All drugs were purchased from Sigma Aldrich, St. Louis, MO, USA.

Statistical analysis

Intra-class correlation coefficients (ICC) and 95% confidence intervals (CIs) were calculated with a two-way mixed-effects model. The reliability coefficient, which is the difference value that will be exceeded by only 5% of pairs of measurements on the same subject, was calculated as 1.96 times the standard deviation (SD) of the difference between pairs of repeated measurements [33].

All remaining statistical analysis used only non-parametric techniques. Sample correlations were evaluated by the Spearman rank correlation coefficient. The statistical significance of the difference between the medians of a continuous variable in two disjoint groups was assessed by the Mann–Whitney test. Clustering of longitudinal PI data were obtained from the application of the K-means algorithm implemented with the Euclidean distance [34].

The clustering algorithm was run several times considering 40 different starting conditions and varying the number of clusters from 2 to 3. Varying the initial conditions increased the chances of reaching a global maximum whereas varying the number of clusters enabled the selection of the correct number of clusters. The sample size was the main reason for the upper bound of the number of clusters used in this paper. The final clustering structure was chosen based upon the clinical interpretation of the obtained groups and the statistical criteria of Calinsky & Harabatz and Davies & Bouldin [35].

Clustering was performed on the group of PI individual time profiles, and separately for each evaluated artery. The NOX activity within each obtained class was then identified and comparisons across clusters were also considered. This procedure was thought to be more informative than simply studying the correlations between each enzymatic activity and the PI values collected at each of the evaluation periods.

All statistical analyses were performed using the R language and software environment for statistical computation, version 2.12.1 [36]. The significance level was set at 0.05.

Results

A total of 19 pregnant women at term were considered eligible for this study according to the established inclusion/exclusion criteria, and their characteristics and pregnancy outcomes are depicted in Table 1. Their ages ranged from 22 to 41 years old, and this was the first pregnancy for 74% of the women.

The median gestational age at the time of Doppler measurements was 21.0 weeks (range: 20–22 weeks) at the first time point and 40.6 weeks (range: 40–41 weeks) at the second time point.

Table 1
Characteristics and obstetric data of the 19 women included in the study.

		N (%)
Age, years (mean, SD)	31.2 (5.0)	
Parity	0	14 (74%)
	> 0	5 (26%)
Body Mass Index, kg/m^2 (mean, SD)[a]	30.6 (5.9)	
Smoking	No	18 (95%)
	Yes	1 (5%)
GA at delivery (weeks) (mean $\pm$ SD)	40.5 (0.3)	
Apgar Index 5′	< 7	0 (0)
Birth weight at delivery (g) (mean $\pm$ SD)[b]	3354 (398)	–

GA, gestational age; SD, standard deviation.

[a] BMI: measured at Caesarean section day.

[b] Birth weight in the sample corresponding to the 10th percentile was 2904 g.
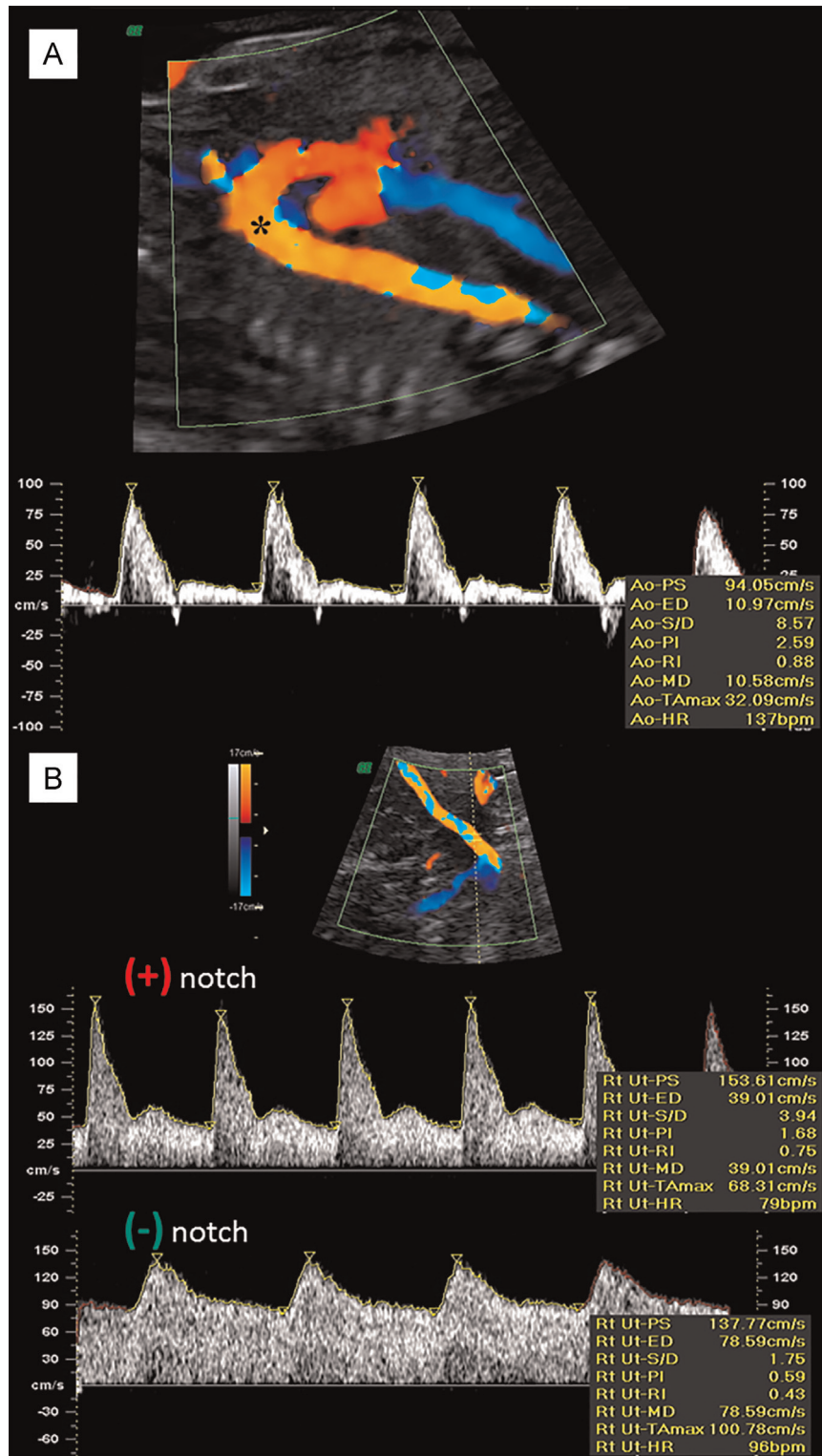
Fig. 1. Doppler flow velocity waveforms obtained from the fetal aortic isthmus (panel A) and maternal uterine artery (panel B). panel A: The aortic Isthmus (AoI) is the segment of the aorta located between the origin of the left subclavian artery and the connection of the ductus arteriosus to the descending aorta (*). Under physiological conditions, the direction of flow in the AoI is forward during the entire cardiac cycle. panel B: With the advent of color Doppler, the precise localization of the uterine arteries became feasible; (+) notch, abnormal waveform demonstrating increased impedance and early diastolic notch; (−) notch, normal pregnant waveform.

Fig. 1 shows the types of AoI and UtA Doppler shift spectra obtained from the fetal aortic isthmus and maternal uterine arteries. The reliability coefficient for the UtA-PI measurements was 0.102. The ICC for absolute agreement among the single observer UtA-PI measurements was 0.990 with a 95% CI ranging from 0.980 to 0.995. Similarly, the reliability coefficient for the

AoI-PI measurements was 0.302. The ICC for absolute agreement among the single observer measurements was 0.976 with a 95% CI ranging from 0.954 to 0.987.

Fig. 2 shows how the biopsies in the placenta and placental bed were obtained.
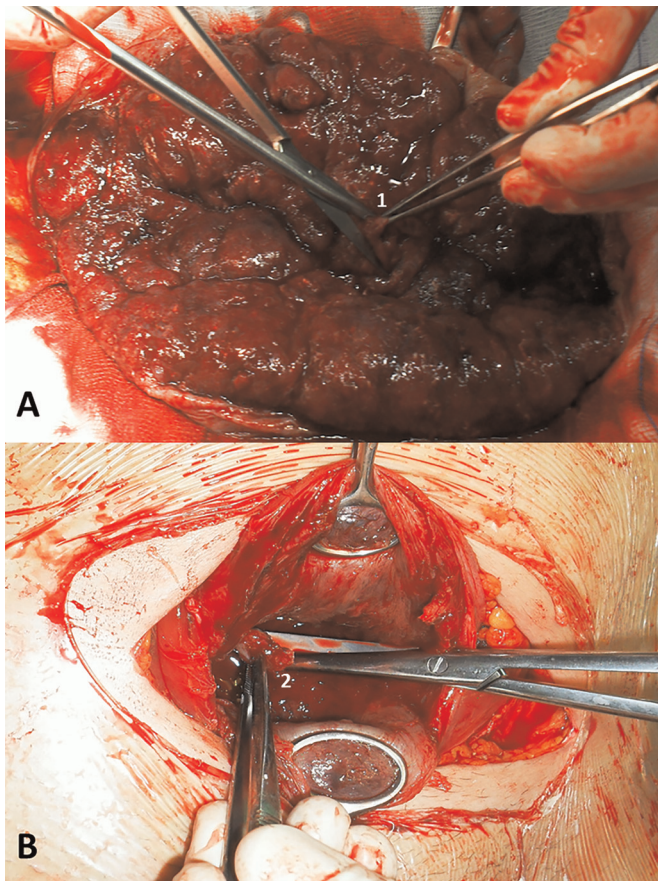
Fig. 2. Placental and placental bed biopsies. (A) Placenta, central maternal surface (1); (B) placental bed (2).

The association between DHE-conversion and PI values (Fig. 3) was first studied using Spearman correlation. From Table 2, AoI-PI and the UtA-PI are positively associated with DHE-conversion (both in the placental bed and in the placenta). In the placental bed, the positive association between DHE-conversion and AoI-PI at the first evaluation period is only statistically significant at the 0.09 level ($p=0.08$), and no significant association exists with AoI-PI at the second evaluation period ($p=0.44$). However, when measured in placental tissue, DHE-conversion showed a significantly positive association with AoI-PI at second time point ($p<0.01$), but not at the first time point ($p=0.164$). There is a significant positive association between DHE-conversion at the placental bed and UtA-PI at the first and second time points, with a stronger association at the first time point. The enzymatic activity of placental DHE-conversion was found to be significantly and positively associated with UtA-PI only at the first time point ($p=0.023$). The positive UtA-PI association with placental bed DHE-conversion at the first time point was 44% higher than the association observed with placental DHE-conversion.

Clustering the individual time profiles to analyze PI values at the AoI and UtA independently allowed for the identification of PI trends. DHE-conversion was then compared across the obtained partition of curves. This was used as a more comprehensive methodology than simply considering correlations with PI values at each of the evaluation time points.

For the AoI-PI measurements, two clusters were identified (Fig. 4A): cluster A comprised 10 (52.6%) pregnant women and cluster B comprised 9 (47.4%). No significant relationship was found between the clustering obtained and the DHE-conversion measured in the placenta and the placental bed (Fig. 4B, Table 3). When examining the UtA-PI values, two clusters were found

(Fig. 4C): cluster A comprised 13 (68.4%) individuals and cluster B comprised 6 individuals (31.6%). UtA cluster B contained all those trajectories starting at higher UtA-PI values and is significantly associated with enhanced DHE-conversion in the placental bed (Fig. 4D, Table 3). By contrast, the persistence of a notch in the uterine artery at 20–22 weeks of gestation was significantly associated with high DHE-conversion in the placental bed, but not in the placenta (Table 4).

Finally, we found that elevated DHE-conversion correlated negatively with the Body Mass Index (BMI) of pregnant women (Table 5). No significant relationship was found between age and the enzymatic activity studied.

Discussion

During a pregnancy, both the foetus and the mother experience substantial circulatory changes. Provided that vascular congenital abnormalities are absent, the fetal circulation will follow an intrinsic, species-related developmental programme; on the mother's side, the pregnancy will impart to the placental bed a variety of structural and functional changes that result in important circulatory events.

At approximately 8 weeks of gestation, embryo-derived extravillous trophoblasts (EVTs) tend to surround decidual spiral arteries, invade their walls, and assemble as cell plugs that ultimately fill their lumina from 10 weeks onwards [37]. Upon replacing vessel endothelium and the smooth muscle cells, trophoblasts subsequently extend to the innermost myometrium layers and cluster around the spiral arteries. By 14 weeks, deep myometrium involvement is evidenced by the trophoblast invasion of the spiral arteries of the lumina. In time, this remodelling process, deep placentation, will extend to most spiral arteries [14,37].

An important consequence of the remodelled vessel is its enlargement, implying the acquisition of capacitance properties, reduced impedance to blood flow, and reduced uterine artery PI. However, if spiral artery remodelling is defective, the uterine artery maintains resistance properties and its impedance increases. Such changes were found to associate with PE and other obstetrical disorders with adverse implications for maternal and fetal health [13,38,39].

In this context, it is useful to analyze blood flow waveforms and determine the UtA [3,20] and AoI [40] impedance. Although a high AoI-PI is seen as an indicator of placental insufficiency and fetal cardiac decompensation [41], there is substantial evidence that high UtA impedance measured at 20–22 weeks is a good predictor of serious pregnancy disorders and adverse fetal outcomes arising in the following weeks until term [3,20,23,42].

As none of those adverse conditions affected the outcomes of any of the pregnancies enrolled in the current study, both the first and second time-point measurements reflected a normal pregnancy course; as expected [3,17], UtA-PI decreased from the 20–22 week time point until term.

However, a closer analysis found two different clusters of UtA-PI time trajectories, one (B) having a steeper PI reduction and the other (A) showing a flattened PI reduction. This finding indicates that even in the absence of adverse clinical findings or outcomes, coherent, specific UtA impedance trends exist, suggesting the action of local regulatory mechanisms that are fine-tuned at different levels. When vessel remodelling is deficient or when predisposing conditions exist, UtA-PI is likely to increase and to be accompanied by clinical signs. The reason for this consequence of abnormal remodelling is unknown, but the current study supports the view that continued redox imbalance and established oxidative stress is the underlying process.
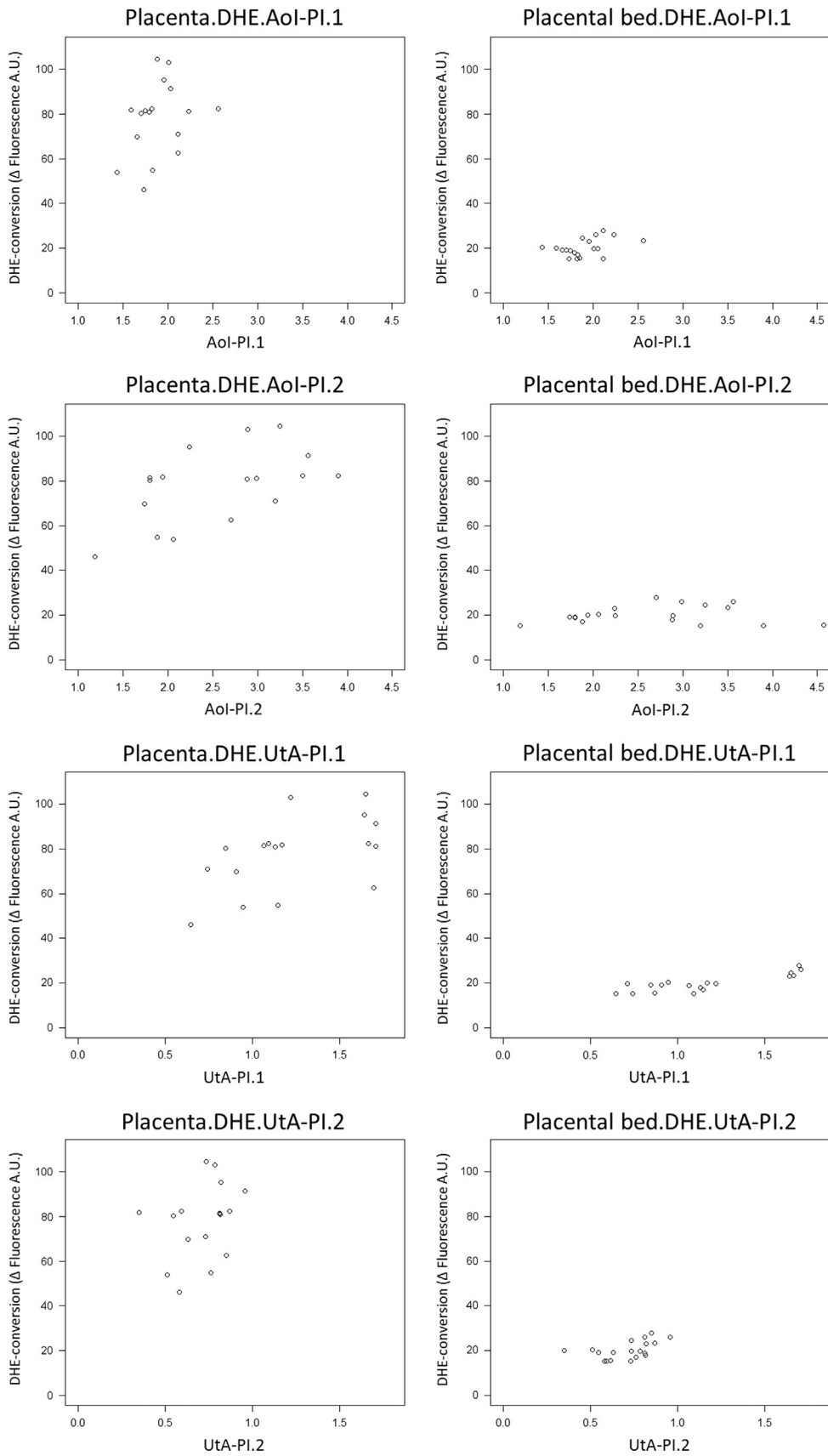
Fig. 3. Plots of the sample values of DHE conversion against AoI-PI and UtA-PI measurements, at the first (1) and second (2) time points, in the placenta and in the placental bed (respectively, left and right columns).

Table 2
Association between DHE-conversion activity and longitudinal AoI-PI and UtA-PI values at the first (1) and second (2) time points.

|	AoI-PI.1	AoI-PI.2	UtA-PI.1	UtA-PI.2
DHE-conversion(Δ Fluorescence A.U.)				
Placenta	0.353	**0.612**	**0.548**	0.357
($n=17$)	($p=0.164$)	($p=0.009$)	($p=0.023$)	($p=0.160$)
Placental bed	0.409	0.187	**0.789**	**0.501**
($n=19$)	($p=0.082$)	($p=0.444$)	($p<0.001$)	($p=0.029$)

AoI, aortic isthmus; UtA, uterine artery; PI, pulsatility index; A.U., arbitrary units

Statistics

The high magnitude of the obtained ICC values from AoI and UtA Doppler assessments allowed statistical analysis to ignore one of the two measurements obtained from each woman. Because the sonographer only performed one measurement in day-to-day practice, the first measurements were considered. Both left and right main UtAs were investigated at the same time, as unilateral measurement may provide erroneous results.

Clustering methods besides k-means could have been chosen for the identification of homogeneous classes of individual PI trajectories. More precisely, hierarchical methods, density-based methods, grid-based methods, model-based methods, or other partitioning methods could have been considered [43]. However, the following points illustrate the advantages of the longitudinal k-means algorithm: (1) it does not require any normality or parametric assumptions within clusters; this is particularly important in our study given its sample size and the fact that no prior information was available; (2) it does not require any assumptions regarding the shape of the individual trajectories; and (3) it is independent from the time scaling used. In this study, the clustering of the linear AoI-PI time profiles into 3 classes provided a group consisting of only 2 individuals and that was therefore discarded. Although the 3-cluster solution for UtA-PI longitudinal profiles presented essentially balanced group prevalence (7, 6, and 6 members), it was not favored by the statistical criteria. No significant association was found between the profile partitions obtained for AoI and NOX activity. Although one of the clusters presented a small dispersion of values and seemed to be well-identified from that point of view, the other included a wide range of enzymatic expression values. The 3-cluster solution mentioned above was not capable of solving this lack of correlation.
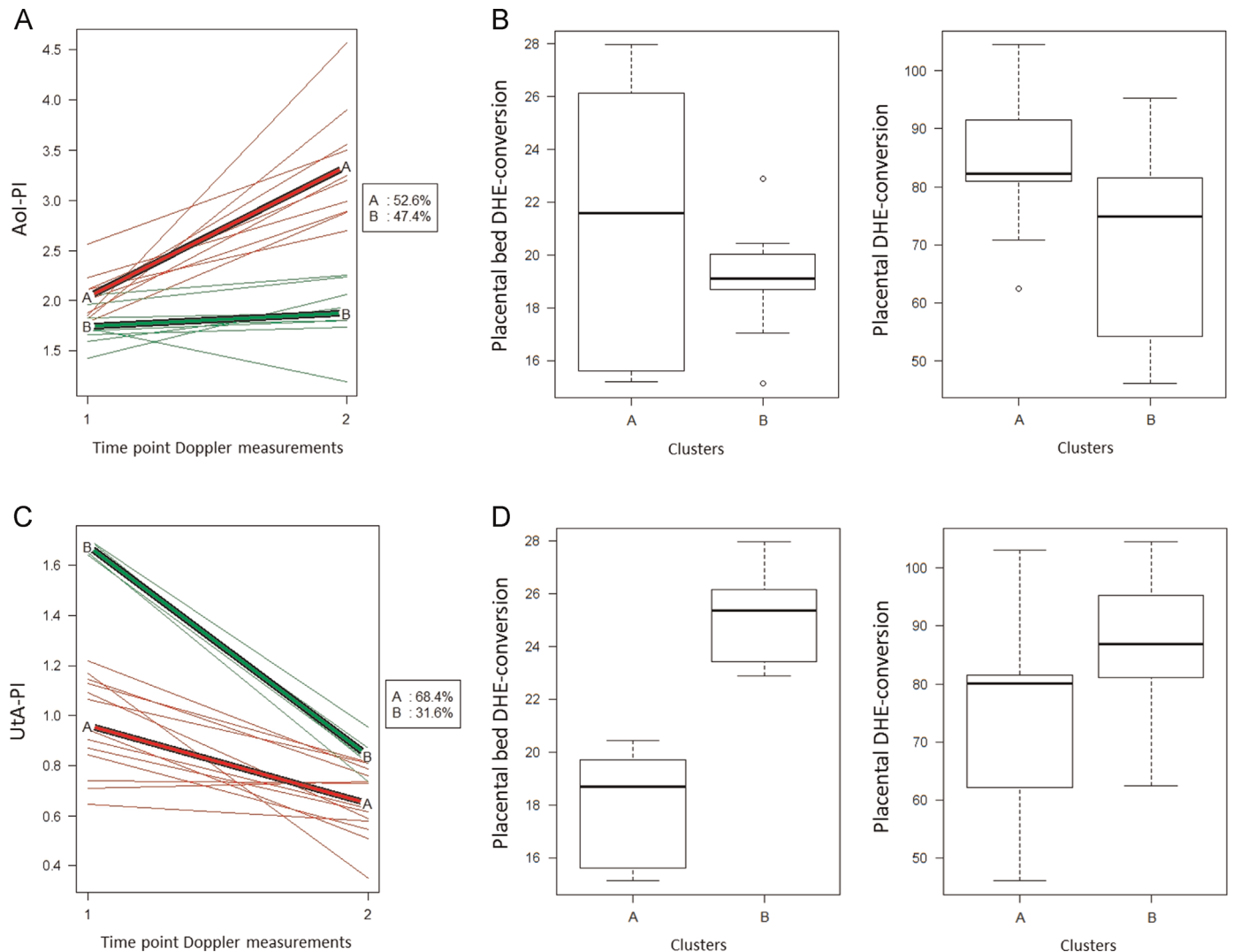
Fig. 4. Panel A+C: individual time profiles of the AoI-PI and UtA-PI (left-hand side) and the two identified clusters, denoted by A and B; all curves in red belong to the A cluster whereas all curves in green belong to the B cluster. Panel B + D: boxplot of placental bed and placental DHE-conversion in each of the clusters found for the AoI-PI and UtA-PI time trajectories.

Table 3
Median (minimum–maximum) placental bed and placental DHE-conversion in each of the clusters (A and B) found for the AoI-PI and UtA-PI time trajectories.

	All	AoI.Cluster A	AoI.Cluster B	p	UtA.Cluster A	UtA.Cluster B	p
DHE-conversion (Δ Fluorescence A.U.)							
Placenta (n=17)	81.08 (46.12–104.52)	82.26 (62.50–104.52)	74.96 (46.12–95.22)	0.093	80.16 (46.12–103.09)	86.89 (62.50–104.52)	0.098
Placental bed (n=19)	19.72 (15.14–27.98)	21.59 (15.21–27.98)	19.13 (15.14–22.91)	0.400	18.72 (15.14–20.47)	25.39 (22.91–27.98)	**< 0.001**

p-Value from the Mann–Whitney test; AoI, aortic isthmus; UtA, uterine artery

Table 4
Median (minimum–maximum) placental bed and placental DHE-conversion in relation to the presence/absence of UtA notching (at the first time point) and parity.

	All	UtA.Notch (−)	UtA.Notch (+)	p	Primiparous	Parous	p
DHE- conversion (Δ Fluorescence A.U.)							
Placenta (n=17)	81.08 (46.12–104.52)	75.52 (46.12–103.09)	82.26 (62.50–104.52)	0.070	81.41 (46.12–103.09)	74.96 (54.71–104.52)	0.703
Placental bed (n=19)	19.72 (15.14–27.98)	18.29 (15.14–20.47)	24.64 (20.05–27.98)	**< 0.001**	19.89 (15.14–27.98)	19.01 (15.63–24.64)	0.500

p-Value from the Mann–Whitney test, UtA, uterine artery.

Table 5
Spearman rank correlation coefficient (*p*-value) between age/BMI and DHE-conversion in the placental bed and in the placenta.

	Age	BMI[1]
DHE-conversion (Δ Fluorescence A.U.)		
Placenta (n=17)	0.081 (0.757)	−0.277 (0.281)
Placental bed (n=19)	0.158 (0.519)	**−0.465 (0.047)**

[a] Measured at the second time point; BMI, Body Mass Index.

NOX activity at the placental bed and Doppler flow study

The structural and functional integrity of the vascular system of the placental bed is controlled by the endothelium [44]. Endothelial cells produce a vast number of circulation regulators that modulate signalling pathways whose activation requires balanced ROS action [45]. In the uterus and placenta, substantial ROS production is the result of NOX activity through its NOX1, NOX2, NOX4, and NOX5 isoforms present in the endothelium, the myometrium smooth muscle cells, the decidualized stromal cells, and the syncytiotrophoblasts, where they generate H_2O_2 and superoxide anions [24,46,47].

The balanced production of ROS has local signalling properties through the synthesis of nitric oxide, NO [48], a primary endothelial cell vasodilator that is critical for endothelium transformation during pregnancy [49].

However, the balance may be disrupted when local conditions enhance NOX activity and ROS production and lead to vessel disorders. In human vascular samples, NOX-dependent superoxide generation and abnormal endothelium-related responses were found to correlate positively with the number of cardiovascular risk factors present [50]. Aortic samples from NOX2 knockout mice failed to respond to hypertensive experiments or to hypotensive challenging as a result of a substantial reduction in superoxide production [51]; interestingly, transgenic mice overexpressing endothelial cell NOX2 exhibited basal activity similar to controls but demonstrated remarkable sensitivity when challenged with angiotensin II [52]. This is an important finding because the involvement of this vasoactive peptide in pregnancy-induced hypertensive disorders has long been recognized [53] and has been interpreted as resulting from enhanced sensitivity [54].

As NOX production of superoxide anions intensifies in smooth muscle cells and human trophoblasts, persistent NF-kB activation ensues [55], which reduces NO bioavailability. This set of conditions promotes local inflammation and further oxidation, both consistently implicated in the pathogenesis of the endothelial dysfunction antedating PE and other disorders at the utero-placental interface [44,54,56,57].

In the current study involving pregnancies that followed a normal course, a validated DHE-based fluorescence method was used as an indicator of NOX activity. Higher placental bed NOX activity related DHE conversion at term was strongly correlated with higher UtA-PI measured at 20–22 weeks (and at term) and also correlated significantly with notch persistence; as only AoI-PI at term was significant, the placental correlations are weaker, emphasizing the value of UtA-PI as previously reported [39,42]. It is uncertain whether fetal changes are independent of placental bed redox modifications or are secondary to these modifications because the foetoplacental unit is reliant on uterine artery perfusion. The finding of a negative correlation between NOX activity at the placental bed (but not at the placenta) and BMI is surprising in view of the general recognition that obesity is associated with oxidative stress [58]. However, this correlation may reflect only a particular local regulation as adipocytes produce a variety of peptides with modulatory abilities, including adiponectin, which was found to down-regulate NOX activity [59,60].

We are convinced that the same mechanisms that enhance placental bed NOX activity related DHE conversion in the identified clusters are able to maintain higher UtA-PI in the same clusters. Therefore, considering the strong correlation between the higher levels of UtA-PI at 20–22 weeks and NOX activity in the uterine tissue at term, it is conceivable that, should UtA-PI become even higher, enhanced NOX activity would increase in a parallel fashion. Eventually, excessive local oxidation would result in abnormally high UtA-PI and unfavourable clinical outcomes; that is, the intensity of the oxidative insult would mark the distinction between functional disturbance and disease.

Although this study does not present placental bed NOX as a disorder biomarker, it provides strong evidence that, at both the uterus and the placenta, NOX is an important intervenient in the redox balance at the human fetal–maternal interface. Further knowledge of its regulation will provide useful insight for the better management of hypertensive disorders of pregnancy.

Study limitations and future research

The longitudinal k-means algorithm also suffers from some drawbacks [34]. (1) There are no formal hypothesis tests to check the validity of the partition. (2) The number of clusters must be known a priori. (3) The algorithm convergence to a global maximum is not assured, and therefore one cannot be sure that the best partition has been found. Another obvious limitation of the statistical analysis in this study was its sample size. A larger sample size would allow for the application of (semi-)parametric models (such as finite mixture models for clustering and *t*-tests for the evaluation of enzymatic activities within the clusters), which are known to be less conservative than non-parametric approaches (4). The intervention of other ROS producers and ROS scavengers was not studied, thus limiting the interpretation of the role of other ROS producers and antioxidant molecules.

Conclusions

This study provides evidence that in normal pregnancies, there is an important involvement of NOX mediated superoxide production, at the fetal/maternal interface. Notably, it was the placental bed that exhibited stronger positive correlation between NOX activity and UtA-PI.

Authors' contributions

G-M. designed the study, performed all Doppler measurements, collected the placenta/placental bed samples, analyzed the data, and wrote the manuscript; E.S. designed the study, coordinated all laboratorial experiments, analyzed the data, and composed the manuscript; A.R.G. performed all statistical analyses; J.P.S. contributed to the critical revision of the manuscript and coordinated the review of clinical cases; A.I.S. and J.A. participated in laboratory experiments; F.M. designed the study and contributed to the critical revision of the manuscript; H.A. designed the study, contributed to supervision, analyzed the data, and wrote the manuscript. All authors contributed to data interpretation and the final version of the manuscript, which all approved.

Conflict of interest

The authors declare no conflicts of interest.

Acknowledgements

Appendix A. Supporting information

Supplementary data associated with this article can be found in the online version at http://dx.doi.org/10.1016/j.jbiomech.2015.03.029.

References

[1] C. Hoffman, H.L. Galan, Assessing the 'at-risk' fetus: Doppler ultrasound, Current Opinion in Obstetrics and Gynecology 21 (2) (2009) 161–166. http://dx.doi.org/10.1097/GCO.0b013e3283292468 19996868.

[2] T. Stampalija, G.M. Gyte, Z. Alfirevic, Utero-placental Doppler ultrasound for improving pregnancy outcome, Cochrane Database of Systematic Reviews 9 (9) (2010) CD008363. http://dx.doi.org/10.1002/14651858.CD008363.pub2 20824875.

[3] O. Gómez, F. Figueras, S. Fernández, M. Bennasar, J.M. Martínez, B. Puerto, E. Gratacós, Reference ranges for uterine artery mean pulsatility index at 11–41 weeks of gestation, Ultrasound in Obstetrics and Gynecology 32 (2) (2008) 128–132. http://dx.doi.org/10.1002/uog.5315 18457355.

[4] G. Acharya, Technical aspects of aortic Isthmus Doppler velocimetry in human fetuses, Ultrasound in Obstetrics and Gynecology 33 (6) (2009) 628–633. http://dx.doi.org/10.1002/uog.6406 19479680.

[5] J. Ruskamp, J.C. Fouron, J. Gosselin, M.J. Raboisson, C. Infante-Rivard, F. Proulx, Reference values for an index of fetal aortic isthmus blood flow during the second half of pregnancy, Ultrasound in Obstetrics and Gynecology 21 (5) (2003) 441–444. http://dx.doi.org/10.1002/uog.105 12768553.

[6] J.C. Fouron, J. Gosselin, M.J. Raboisson, J. Lamoureux, C.A. Tison, C. Fouron, L. Hudon, The relationship between an aortic isthmus blood flow velocity index and the postnatal neurodevelopmental status of fetuses with placental circulatory insufficiency, American Journal of Obstetrics and Gynecology 192 (2) (2005) 497–503. http://dx.doi.org/10.1016/j.ajog.2004.08.026 15695993.

[7] S.E. Sonesson, J.C. Fouron, Doppler velocimetry of the aortic isthmus in human fetuses with abnormal velocity waveforms in the umbilical artery, Ultrasound in Obstetrics and Gynecology 10 (2) (1997) 107–111. http://dx.doi.org/10.1046/j.1469-0705.1997.10020107.x 9286019.

[8] K. Mäkikallio, P. Jouppila, J. Räsänen, Retrograde net blood flow in the aortic isthmus in relation to human fetal arterial and venous circulations, Ultrasound in Obstetrics and Gynecology 19 (2) (2002) 147–152. http://dx.doi.org/10.1046/j.0960-7692.2001.00626.x 11876806.

[9] K. Mäkikallio, P. Jouppila, J. Räsänen, Retrograde aortic isthmus net blood flow and human fetal cardiac function in placental insufficiency, Ultrasound in Obstetrics and Gynecology 22 (4) (2003) 351–357. http://dx.doi.org/10.1002/uog.232 14528469.

[10] G. Rizzo, A. Capponi, M. Vendola, M.E. Pietrolucci, D. Arduini, Relationship between aortic isthmus and ductus venosus velocity waveforms in severe growth restricted fetuses, Prenatal Diagnosis 28 (11) (2008) 1042–1047. http://dx.doi.org/10.1002/pd.2121 18973156.

[11] M. Del Río, J.M. Martínez, F. Figueras, M. Bennasar, A. Olivella, M. Palacio, O. Coll, B. Puerto, E. Gratacós, Doppler assessment of the aortic isthmus and perinatal outcome in preterm fetuses with severe intrauterine growth restriction, Ultrasound in Obstetrics and Gynecology 31 (1) (2008) 41–47. http://dx.doi.org/10.1002/uog.5237 18157796.

[12] K. Mäkikallio, Is it time to add aortic isthmus evaluation to the repertoire of Doppler investigations for placental insufficiency? Ultrasound in Obstetrics and Gynecology 31 (1) (2008) 6–9. http://dx.doi.org/10.1002/uog.5239 18098344.

[13] S. Lin, I. Shimizu, N. Suehara, M. Nakayama, T. Aono, Uterine artery Doppler velocimetry in relation to trophoblast migration into the myometrium of the placental bed, Obstetrics and Gynecology 85 (5 Pt 1) (1995) 760–765. http://dx.doi.org/10.1016/0029-7844(95)00020-R 7724109.

[14] I. Brosens, R. Pijnenborg, L. Vercruysse, R. Romero, The "Great obstetrical syndromes" are associated with disorders of deep placentation, American Journal of Obstetrics and Gynecology 204 (3) (2011) 193–201. http://dx.doi.org/10.1016/j.ajog.2010.08.009 21094932.

[15] C.V. Steer, J. Williams, J. Zaidi, S. Campbell, S.L. Tan, Intra-observer, inter-observer, interultrasound transducer and intercycle variation in colour Doppler assessment of uterine artery impedance, Human Reproduction 10 (2) (1995) 479–481 7769083.

[16] L. Guedes-Martins, J. Saraiva, R. Gaio, F. Macedo, H. Almeida, Uterine artery impedance at very early clinical pregnancy, Prenatal Diagnosis 34 (8) (2014) 719–725. http://dx.doi.org/10.1002/pd.4325 24431243.

[17] L. Guedes-Martins, A. Cunha, J. Saraiva, R. Gaio, F. Macedo, H. Almeida, Internal iliac and uterine arteries Doppler ultrasound in the assessment of normotensive and chronic hypertensive pregnant women, Scientific Reports 4 (2014) 3785. http://dx.doi.org/10.1038/srep03785 24445576.

[18] A.T. Papageorghiou, C.K. Yu, R. Bindra, G. Pandis, K.H. Nicolaides, Fetal Medicine Foundation Second Trimester Screening Group, Multicenter screening for pre-eclampsia and fetal growth restriction by transvaginal uterine artery Doppler at 23 weeks of gestation, Ultrasound in Obstetrics and Gynecology 18 (5) (2001) 441–449. http://dx.doi.org/10.1046/j.0960-7692.2001.00572.x 11844162.

[19] A.T. Papageorghiou, C.K. Yu, I.E. Erasmus, H.S. Cuckle, K.H. Nicolaides, Assessment of risk for the development of pre-eclampsia by maternal characteristics and uterine artery Doppler, BJOG 112 (6) (2005) 703–709. http://dx.doi.org/10.1111/j.1471-0528.2005.00519.x 15924523.

[20] H.J. van den Elzen, T.E. Cohen-Overbeek, D.E. Grobbee, R.W. Quartero, J. W. Wladimiroff, Early uterine artery Doppler velocimetry and the outcome of pregnancy in women aged 35 years and older, Ultrasound in Obstetrics and Gynecology 5 (5) (1995) 328–333. http://dx.doi.org/10.1046/j.1469-0705.1995.05050328.x 7614138.

[21] M.W. Aardema, M.C. Saro, M. Lander, B.T. De Wolf, H. Oosterhof, J. G. Aarnoudse, Second trimester Doppler ultrasound screening of the uterine arteries differentiates between subsequent normal and poor outcomes of hypertensive pregnancy: two different pathophysiological entities? Clinical Science 106 (4) (2004) 377–382. http://dx.doi.org/10.1042/CS20030385 14636154.

[22] G.C. Smith, C.K. Yu, A.T. Papageorghiou, A.M. Cacho, K.H. Nicolaides, Fetal Medicine Foundation Second Trimester Screening Group, Maternal uterine artery Doppler flow velocimetry and the risk of stillbirth, Obstetrics and Gynecology 109 (1) (2007) 144–151. http://dx.doi.org/10.1097/01.AOG.0000248536.94919.e3 17197600.

[23] J.S. Cnossen, R.K. Morris, G. ter Riet, B.W. Mol, J.A. van der Post, A. Coomarasamy, A.H. Zwinderman, S.C. Robson, P.J. Bindels, J. Kleijnen, K. S. Khan, Use of uterine artery Doppler ultrasonography to predict preeclampsia and intrauterine growth restriction: a systematic review and bivariable meta-analysis, CMAJ 178 (6) (2008) 701–711. http://dx.doi.org/10.1503/cmaj.070430 18332385.

[24] K. Bedard, K.H. Krause, The NOX family of ROS-generating NADPH oxidases: physiology and pathophysiology, Physiological Reviews 87 (1) (2007) 245–313. http://dx.doi.org/10.1152/physrev.00044.2005 17237347.

[25] J.M. Davis, R.L. Auten, Maturation of the antioxidant system and the effects on preterm birth, Seminars in Fetal and Neonatal Medicine 15 (4) (2010) 191–195. http://dx.doi.org/10.1016/j.siny.2010.04.001 20452845.

[26] T. Cindrova-Davies, H.W. Yung, J. Johns, O. Spasic-Boskovic, S. Korolchuk, E. Jauniaux, G.J. Burton, D.S. Charnock-Jones, Oxidative stress, gene expression, and protein changes induced in the human placenta during labor, American Journal of Pathology 171 (4) (2007) 1168–1179. http://dx.doi.org/10.2353/ajpath.2007.070528 17823277.

[27] G.J. Burton, E. Jauniaux, D.S. Charnock-Jones, The influence of the intrauterine environment on human placental development, International Journal of Development Biology 54 (2–3) (2010) 303–312. http://dx.doi.org/10.1387/ijdb.082764gb 19757391.

[28] G.J. Burton, E. Jauniaux, Oxidative stress, Best Practice and Research: Clinical Obstetrics and Gynaecology 25 (3) (2011) 287–299. http://dx.doi.org/10.1016/j.bpobgyn.2010.10.016 21130690.

[29] H.P. Robinson, Sonar measurement of fetal crown-rump length as means of assessing maturity in first trimester of pregnancy, British Medicine Jounal 4 (5883) (1973) 28–31 4755210.

[30] T. Sousa, D. Pinho, M. Morato, J. Marques-Lopes, E. Fernandes, J. Afonso, S. Oliveira, F. Carvalho, A. Albino-Teixeira, Role of superoxide and hydrogen peroxide in hypertension induced by an antagonist of adenosine receptors, European Journal of Pharmacology 588 (2–3) (2008) 267–276. http://dx.doi.org/10.1016/j.ejphar.2008.04.044 18519134.

[31] X.Y. Yi, V.X. Li, F. Zhang, F. Yi, D.R. Matson, M.T. Jiang, P.L. Li, Characteristics and actions of NAD(P)H oxidase on the sarcoplasmic reticulum of coronary artery smooth muscle, American Journal of Physiology: Heart and Circulatory Physiology 290 (3) (2006) H1136–H1144. http://dx.doi.org/10.1152/ajpheart.00296.2005 16227345.

[32] M.M. Bradford, A rapid and sensitive method for the quantitation of microgram quantities of protein utilizing the principle of protein-dye binding, Analytical Biochemistry 72 (1976) 248–254. http://dx.doi.org/10.1016/0003-2697(76)90527-3 942051.

[33] J.M. Bland, D.G. Altman, Applying the right statistics: analyses of measurement studies, Ultrasound in Obstetrics and Gynecology 22 (1) (2003) 85–93. http://dx.doi.org/10.1002/uog.122 12858311.

[34] C. Genolini, B. Falissard, KmL: k-means for longitudinal data, Computional Statistics 25 (2) (2010) 317–328. http://dx.doi.org/10.1007/s00180-009-0178-4.

[35] U. Maulik, S. Bandyopadhyay, Performance evaluation of some clustering algorithms and validity indices, IEEE Transaction on Pattern Analysis and Machine Intelligence 24 (12) (2002) 1650–1654. http://dx.doi.org/10.1109/TPAMI.2002.1114856.

[36] R. Development Core Team R: A language and environment for statistical computing R Foundation for Statistical Computing, Vienna, Austria, 2010. Available at: http://www.R-project.org/ (accessed 18.06.13).

[37] R. Pijnenborg, L. Vercruysse, I. Brosens, Deep placentation, Best Practice and Research: Clinical Obstetrics and Gynaecology 25 (3) (2011) 273–285. http://dx.doi.org/10.1016/j.bpobgyn.2010.10.009 21212025.

[38] S. Sağol, E. Ozkinay, K. Oztekin, N. Ozdemir, The comparison of uterine artery Doppler velocimetry with the histopathology of the placental bed, Australian and New Zealand Journal of Obstetrics and Gynaecology 39 (3) (1999) 324–329. http://dx.doi.org/10.1111/j.1479-828X.1999.tb03407.x 10554944.

[39] R. Madazli, A. Somunkiran, Z. Calay, S. Ilvan, M.F. Aksu, Histomorphology of the placenta and the placental bed of growth restricted foetuses and correlation with the Doppler velocimetries of the uterine and umbilical arteries, Placenta 24 (5) (2003) 510–516. http://dx.doi.org/10.1053/plac.2002.0945 12744927.

[40] M.M. Kennelly, N. Farah, M.J. Turner, B. Stuart, Aortic Isthmus Doppler velocimetry: role in assessment of preterm fetal growth restriction, Prenatal Diagnosis 30 (5) (2010) 395–401. http://dx.doi.org/10.1002/pd.2474 20232481.

[41] F. Figueras, A. Benavides, M. Del Del Rio, F. Crispi, E. Eixarch, J.M. Martinez, E. Hernandez-Andrade, E. Gratacós, Monitoring of fetuses with intrauterine growth restriction: longitudinal changes in ductus venosus and aortic isthmus flow, Ultrasound in Obstetrics and Gynecology 33 (1) (2009) 39–43. http://dx.doi.org/10.1002/uog.6278 19115231.

[42] M.W. Aardema, H. Oosterhof, A. Timmer, I. van Rooy, J.G. Aarnoudse, Uterine artery Doppler flow and uteroplacental vascular pathology in normal pregnancies and pregnancies complicated by pre-eclampsia and small for gestational age foetuses, Placenta 22 (5) (2001) 405–411. http://dx.doi.org/10.1053/plac.2001.0676 11373150.

[43] T. Warren Liao, Clustering of time series data – a survey, Pattern Recognition 38 (11) (2005) 1857–1874. http://dx.doi.org/10.1016/j.patcog.2005.01.025.

[44] L. Guedes-Martins, L. Matos, A. Soares, E. Silva, H. Almeida, AGEs, contributors to placental bed vascular changes leading to preeclampsia, Free Radical Research 47 (Suppl. 1) (2013) S70–S80. http://dx.doi.org/10.3109/10715762.2013.815347 23796030.

[45] J.D. Lambeth, Nox enzymes, ROS, and chronic disease: an example of antagonistic pleiotropy, Free Radical Biology and Medicine 43 (3) (2007) 332–347. http://dx.doi.org/10.1016/j.freeradbiomed.2007.03.027 17602948.

[46] X.L. Cui, B. Chang, L. Myatt, Expression and distribution of NADPH oxidase isoforms in human myometrium − role in angiotensin II-induced hypertrophy, Biology of Reproduction 82 (2) (2010) 305–312. http://dx.doi.org/10.1095/biolreprod.109.080275 19812300.

[47] R. Lim, R. Acharya, P. Delpachitra, S. Hobson, C.G. Sobey, G.R. Drummond, E. M. Wallace, Activin and NADPH-oxidase in preeclampsia: insights from in vitro and murine studies, American Journal of Obstetrics and Gynecology 212 (1) (2015) 86.e1–86.e12. http://dx.doi.org/10.1016/j.ajog.2014.07.021 25046804.

[48] S.R. Thomas, K. Chen, J.F. Keaney, Hydrogen peroxide activates endothelial nitric-oxide synthase through coordinated phosphorylation and dephosphorylation via a phosphoinositide 3-kinase-dependent signaling pathway, Journal of Biological Chemistry 277 (8) (2002) 6017–6024. http://dx.doi.org/10.1074/jbc.M109107200 11744698.

[49] T.R. Everett, C.C. Lees, Beyond the placental bed: placental and systemic determinants of the uterine artery Doppler waveform, Placenta 33 (11) (2012) 893–901. http://dx.doi.org/10.1016/j.placenta.2012.07.011 22902007.

[50] T.J. Guzik, N.E. West, E. Black, D. McDonald, C. Ratnatunga, R. Pillai, K. M. Channon, Vascular superoxide production by NAD(P)H oxidase: association with endothelial dysfunction and clinical risk factors, Circulation Research 86 (9) (2000) E85–E90 10807876.

[51] O. Jung, J.G. Schreiber, H. Geiger, T. Pedrazzini, R. Busse, R.P. Brandes, gp91phox-containing NADPH oxidase mediates endothelial dysfunction in renovascular hypertension, Circulation 109 (14) (2004) 1795–1801. http://dx.doi.org/10.1161/01.CIR.0000124223.00113.A4 15037533.

[52] C.E. Murdoch, S.P. Alom-Ruiz, M. Wang, M. Zhang, S. Walker, B. Yu, A. Brewer, A.M. Shah, Role of endothelial Nox2 NADPH oxidase in angiotensin II-induced hypertension and vasomotor dysfunction, Basic Research in Cardiology 106 (4) (2011) 527–538. http://dx.doi.org/10.1007/s00395-011-0179-7 21528437.

[53] N.F. Gant, G.L. Daley, S. Chand, P.J. Whalley, P.C. MacDonald, A study of angiotensin II pressor response throughout primigravid pregnancy, Journal of Clinical Investigation 52 (11) (1973) 2682–2689. http://dx.doi.org/10.1172/JCI107462 4355997.

[54] S. Sankaralingam, I.A. Arenas, M.M. Lalu, S.T. Davidge, Preeclampsia: current understanding of the molecular basis of vascular dysfunction, Expert Reviews in Molecular Medicine 8 (3) (2006) 1–20. http://dx.doi.org/10.1017/S1462399406010465 16438753.

[55] R. Dechend, C. Viedt, D.N. Müller, B. Ugele, R.P. Brandes, G. Wallukat, J.K. Park, J. Janke, P. Barta, J. Theuer, A. Fiebeler, V. Homuth, R. Dietz, H. Haller, J. Kreuzer, F.C. Luft, AT1 receptor agonistic antibodies from preeclamptic patients stimulate NADPH oxidase, Circulation 107 (12) (2003) 1632–1639. http://dx.doi.org/10.1161/01.CIR.0000058200.90059.B1 12668498.

[56] K. Ota, S. Yamagishi, M. Kim, S. Dambaeva, A. Gilman-Sachs, K. Beaman, J. Kwak-Kim, Elevation of soluble form of receptor for advanced glycation end products (sRAGE) in recurrent pregnancy losses (RPL): possible participation of RAGE in RPL, Fertility and Sterility 102 (3) (2014) 782–789. http://dx.doi.org/10.1016/j.fertnstert.2014.06.010 25044082.

[57] L.C. Sánchez-Aranguren, C.E. Prada, C.E. Riaño-Medina, M. Lopez, Endothelial dysfunction and preeclampsia: role of oxidative stress, Frontiers in Physiology 5 (2014) 372. http://dx.doi.org/10.3389/fphys.2014.00372 25346691.

[58] S. Le Lay, G. Simard, M.C. Martinez, R. Andriantsitohaina, Oxidative stress and metabolic pathologies: from an adipocentric point of view, Oxidative Medicine and Cellular Longevity 2014 (2014) 908539. http://dx.doi.org/10.1155/2014/908539 25143800.

[59] F. Jiang, H.K. Lim, M.J. Morris, L. Prior, E. Velkoska, X. Wu, G.J. Dusting, Systemic upregulation of NADPH oxidase in diet-induced obesity in rats, Redox Report 16 (6) (2011) 223–229. http://dx.doi.org/10.1179/174329211X13049558293713 22195989.

[60] Y. Zhang, X.L. Wang, J. Zhao, Y.J. Wang, W.B. Lau, Y.X. Yuan, E.H. Gao, W.J. Koch, X.L. Ma, Adiponectin inhibits oxidative/nitrative stress during myocardial ischemia and reperfusion via PKA signaling, American Journal of Physiology - Endocrinology and Metabolism 305 (12) (2013) E1436–E1443. http://dx.doi.org/10.1152/ajpendo.00445.2013 24129398.